Phonon dispersion of the bcc phase of group-IV metals. III. bcc hafnium

J. Trampenau
Institut für Metallforschung, Universität Münster, D-4400 Münster, Germany
and Institut Laue-Langevin, 156X, F-38042 Grenoble CEDEX, France

A. Heiming
Institut Laue-Langevin, 156X, F-38042 Grenoble CEDEX, France
and Institut für Festkörperphysik der Universität Wien, G-1020 Wien, Austria

W. Petry, and M. Alba
Institut Laue-Langevin, 156X, F-38042 Grenoble CEDEX, France

C. Herzig
Institut für Metallforschung, Universität Münster, D-4400 Münster, Germany

W. Miekeley
Hahn-Meitner-Institut GmbH, Glienickerstrasse 100, D-1000 Berlin 39, Germany

H. R. Schober
Institut für Festkörperforschung, KFA Jülich, D-5170 Jülich, Germany
(Received 8 November 1990)

The phonon dispersion of the high-temperature bcc phase of Hf has been measured. The dispersion resembles very much those of the other group-IV metals: bcc Ti and bcc Zr. It is dominated by the low-energy L $\frac{2}{3}(1,1,1)$ mode and by the low-energy T_1 $[\xi\xi 0]$ phonon branch with transverse $[1\bar{1}0]$ polarization. These large-amplitude vibrations displace the lattice toward the stacking sequence of the high-pressure ω structure and the low-temperature hcp structure, respectively, and are interpreted as dynamical precursor fluctuations toward these low-symmetry phases within the high-symmetry bcc phase.

I. INTRODUCTION

Hafnium is the heaviest of the group-IV metals Ti, Zr, and Hf, the valence state of which is defined by two d electrons. Its high-temperature bcc structure (β phase) transforms martensitically at 1742 °C to the low-temperature hcp structure (α phase) and, under pressure, it transforms to an also hexagonal, but not closed-packed structure (ω phase). At room temperature, the pressure needed to transform α to ω is of the order of 210 kbar.[1] Whereas Ti and Zr follow the same structural transformation scheme, the actual transition temperatures and pressures in Hf are considerably higher than in its chemical homologs.

This paper reports on measurements of the complete phonon dispersion in bcc Hf and emphasizes the role of low-energy phonons as dynamical precursors of the first-order displacive or martensitic β-to-ω and β-to-α transition. The results are compared to those of bcc Ti (Ref. 2) and bcc Zr (Ref. 3) (hereafter referred to, respectively, as I and II), and a systematics of the phonon dispersion of the bcc phase of three group-IV metals is presented. It is shown that the dynamics of β-Hf follows essentially that of β-Ti and β-Zr. Differences with respect to the damping of the low-energy phonons are noted. The study of the lattice dynamics of all group-IV metals enables us to present a picture of how the martensitic phase transitions are controlled by the vibrational spectra in these substances often cited as model cases.

II. EXPERIMENTAL DETAILS

The martensitic phase transition prevents quenching of high-temperature bcc single crystals to room temperature. Therefore the bcc single crystals have to be grown *in situ* on the spectrometer, orientated, and kept at temperatures above $T_0 = 1742$ °C during the phonon measurements. We have described the crystal-growth and measurement technique in great detail in I[2] and II,[3] and mention here only a few points which are of particular interest for the phonon measurements in the bcc phase of Hf.

The high-purity Hf has been supplied by Teledyne Wah Chang, Albany, New York. The chemical analysis of the most important impurities as given by the supplier is the following: [C] < 30, [H] < 5, [N] = 5, [O] < 50, and [Zr] = 129 (all in wt. ppm). Similar to Ti and Zr, Hf has a high solubility of gaseous impurities like O, N, and C.[4] To avoid accumulation of these impurities, each crystal was never used twice.

Cooled Mo screws were used to fix the ~100-mm-long Hf rods at both ends inside the furnace. Due to a relative low vapor pressure of Hf at the melting point $T_m = 2227$ °C of $\sim 2\times 10^{-3}$ mbar, single crystals could be

grown by the zone-melting technique in ultrahigh vacuum. Natural Hf has a very high neutron-absorption cross section, σ_{abs} ($\lambda = 1.8$ Å) = 104 barn. Therefore thin crystal rods of 5 mm diameter were used. The very high temperatures did not allow one to grow crystals with more than 2 cm in length. In total, measurements were performed on five crystals with different orientations.

All experiments were performed on the 3-axis spectrometer IN8 of the ILL and the instrumental setup was similar to the ones described in I[2] and II.[3] In most cases, 50′-40′ -40′-40′ collimation and a pyrolytic graphite (PG) (002) analyzer were chosen. For the definition of the scattering plane in reciprocal-lattice units (r.l.u.), a lattice parameter for bcc Hf at 1800 °C $a_{bcc} = 3.61$ Å (Ref. 5) was used. Hf has a high incoherent scattering cross section, $\sigma_{inc} = 2.16$ barn, which leads to a considerable isotropic scattering contribution at $\hbar\omega = 0$ and to an inelastic scattering modulated according to the phonon density of state. The latter hindered considerably the interpretation of phonon groups close to the Brillouin-zone boundary.

III. PHONON DISPERSION OF bcc Hf

The phonon dispersion was measured at 1800 °C, i.e., 60 °C above the β-to-α transition temperature T_0 in the main symmetry directions and is shown in Fig. 1. Also some phonons with off-symmetry propagation in $[\xi\,\xi\,2\xi]$ were measured. The so-called T_1 $[\xi\,\xi\,2\xi]$ with a transverse polarization close to $[11\bar{1}]$ could not be measured because no single crystal with a suitable $\{110\}$ scattering plane could be grown. The T_1 $\frac{1}{3}(1,1,2)$ phonon shown in Fig. 1 is identical to the L $\frac{2}{3}(1,1,1)$ phonon and has been measured in a $\{112\}$ scattering plane. For a more detailed discussion of the phonons with $[\xi\,\xi\,2\xi]$ propagation and their q-dependent polarization we refer to the corresponding sections in I[2] and II.[3]

From the measured spectra phonon energies were defined as I and II.[2,3] Gaussian fits were applied to those phonon groups where no width beyond the instrumental resolution was observed. The L $\frac{2}{3}(1,1,1)$ and all transverse phonons with $[\xi\xi 0]$ propagation and $[1\bar{1}0]$ polarization were assumed to be broadened in energy, i.e., measured as a function of energy at constant q and fitted by means of a damped-oscillator function. The fitting procedure includes the convolution with the measured resolution and accounts for the λ-dependent spectrometer sensitivity. All phonon energies, including those measured at different temperatures, are listed in Tables I and II.

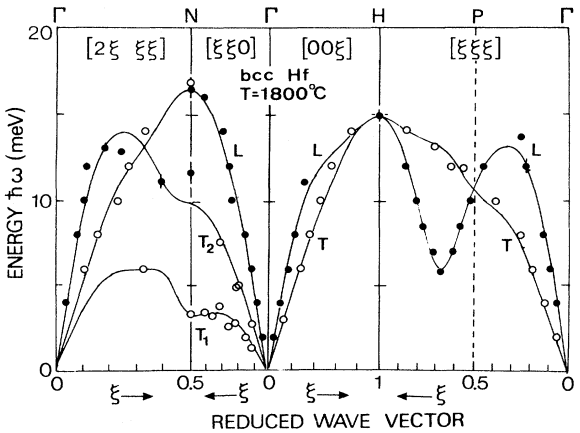

FIG. 1. Phonon dispersion of bcc Hf measured at 1800 °C. The solid line shows a Born-von Kármán fit with force constants up to the fifth nearest neighbor shell.

TABLE I. Phonons in bcc Hf measured at 1800 °C and fitted with a Gaussian line shape.

L $[\xi\xi\xi]$		T $[\xi\xi\xi]$	
ξ	$\hbar\omega$(meV)	ξ	$\hbar\omega$(meV)
0.067(2)	4.0	0.058(1)	2.0
0.099(3)	6.0	0.123(2)	4.0
0.132(5)	8.0	0.190(4)	6.0
0.22(1)	12.0	0.256(3)	8.0
0.25	13.7(2)	0.384(5)	10.0
0.450(5)	12.0	0.55	11.9(4)
0.516(5)	10.0	0.62(1)	12.0
0.569(2)	8.5	0.70	13.1(3)
0.607(3)	7.0	0.85	14.1(4)
0.714(5)	7.0		
0.762(5)	8.5		
0.801(9)	10.0		
0.86(1)	12.0		
1.00	14.9(2)		

L $[00\xi]$		T $[00\xi]$	
ξ	$\hbar\omega$(meV)	ξ	$\hbar\omega$(meV)
0.044(5)	2.0	0.138(3)	3.0
0.108(4)	4.0	0.294(5)	6.0
0.18(1)	6.0	0.37(2)	8.0
0.238(13)	8.0	0.47(3)	10.0
0.33(2)	11	0.57(4)	12.0
		0.75(4)	14.0

L $[\xi\xi 0]$		$T_{[001]}$ $[\xi\xi 0]$	
ξ	$\hbar\omega$(meV)	ξ	$\hbar\omega$(meV)
0.030(1)	2.0	0.1	2.70(4)
0.063(1)	4.0	0.185(4)	5.0
0.100(2)	6.0	0.2	4.9(8)
0.140(2)	8.0	0.3	7.6(3)
0.228(2)	10.0		
0.241(5)	12.0		
0.285(10)	14.0		
0.40(1)	16.0		
0.5	16.4(5)		

L $[\xi\,\xi\,2\xi]$		T_2 $[\xi\,\xi\,2\xi]$	
ξ	$\hbar\omega$(meV)	ξ	$\hbar\omega$(meV)
0.044(1)	4.0	0.113(2)	6.0
0.090(2)	8.0	0.162(4)	8.0
0.105(4)	10.0	0.237(5)	10.0
0.120(4)	10.0	0.280(8)	12.0
0.122(4)	12.0	0.34(3)	14.0
0.19(1)	13.0	0.50	16.8(8)
0.25	12.8(2)		
0.4	11.1(4)		
0.5	11.6(6)		

The phonon dispersion of β-Hf at 1800 °C shows the same anomalies as observed in β-Ti and β-Zr:

(1) The longitudinal phonon branch in [111] direction shows an extreme dip at $\mathbf{q}=\frac{2}{3}(1,1,1)$ and

(2) the whole transverse $[\xi\xi 0]$ phonon branch with $[1\bar{1}0]$ polarization—hereafter called T_1 $[\xi\xi 0]$—is of exceptionally low energy.

All other phonons are of lower energies than the corresponding ones in β-Ti and β-Zr and follow the homology rule[6] $\omega_{Zr}/\omega_{Hf}=(m_{Hf}/m_{Zr})^{1/2}a_{Hf}/a_{Zr}$.

A. The L $\frac{2}{3}(1,1,1)$ phonon

As shown in I and II,[2,3] the L $\frac{2}{3}(1,1,1)$ phonon displaces neighboring (1,1,1) planes toward the structure of the ω phase. From β-Ti and β-Zr, it is known that this phonon is of very low energy. Measurements of the L $\frac{2}{3}(1,1,1)$ phonon in β-Hf at 1800 °C and 2020 °C are shown in Fig. 2 and confirm this picture. A temperature-independent frequency of 5.9(1) meV is found.

TABLE II. Phonons in bcc Hf measured at various temperatures and fitted with a damped oscillator including convolution with the measured resolution and corrections to the wavelength dependent spectrometer sensitivity.

$T_{[1\bar{1}0]}$ $[\xi\xi 0]$		T=1800 °C
ξ	$\hbar\omega$(meV)	Γ(meV)
0.10	1.33(3)	0.0[a]
0.134(2)	2.0	—
0.20	2.8(2)	—[b]
0.25	2.6(2)	—[b]
0.30	3.8(2)	—[b]
0.35	3.23(8)	1.3(2)
0.40	3.42(8)	1.3(2)
0.50	3.34(12)	1.3(3)
$T_{[1\bar{1}0]}$ $[\xi\xi 0]$		T=1950 °C
ξ	$\hbar\omega$(meV)	Γ(meV)
0.10	1.5(1)	0.7[a]
0.130(5)	2.0	—
0.152(3)	2.5	—
0.20	2.45(12)	—[b]
0.325	3.63(6)	2.7(1)
0.35	3.8(1)	2.8(2)
0.40	4.02(8)	2.9(2)
0.45	4.64(13)	3.8(3)
0.50	4.8(2)	4.8(4)
$T_{[1\bar{1}0]}$ $[\xi\xi 0]$		T=2020 °C
ξ	$\hbar\omega$(meV)	Γ(meV)
0.1	1.23(1)	0.0[a]
0.25	3.15(7)	1.6(2)
0.4	5.09(17)	4.6(4)
0.5	5.56(27)	5.5(6)
L $[\xi\xi\xi]$		const Q=(1.35, 1.35, 1.35)
T °C	$\hbar\omega$(meV)	Γ(meV)
1800 °C	5.81(5)	1.6(2)
2020 °C	5.65(10)	4.0(4)

[a] At small q focusing effects are dominant and Gaussian fits were used.

[b] Unreliable fit of the damping due to spurions.

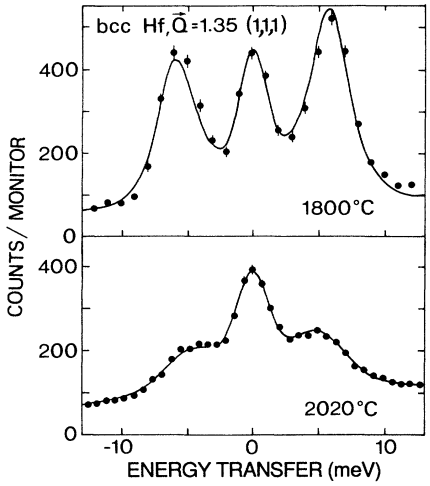

FIG. 2. Energy scan at constant Q=1.35(1,1,1) for two different temperatures in bcc Hf. 50′-40′-40′-40′ collimation, $k_f=4.1$ Å^{-1}, and a PG(002) analyzer have been used. The solid lines show fits with a damped oscillator including a convolution with the resolution, the line shape of which is given by the elastic peak. In this and all following figures the counts have been normalized to the incoming flux (monitor rate=1000).

A comparison of the line shapes of the phonon groups in Fig. 2 reveals two interesting features. Firstly, the L $\frac{2}{3}(1,1,1)$ phonon is broadened with respect to the instrumental resolution indicated by the incoherent elastic peak. Therefore, the appropriate description is a damped oscillator with a damping term $\Gamma=2\hbar/\tau$, which is inversely proportional to the lifetime τ of the phonon. Secondly, Fig. 2 and Table II show that—while the phonon energy $\hbar\omega$ is temperature independent—the damping Γ increases strongly with increasing temperature. The damping is smallest at temperatures close to the β-to-α transition whereas at $T=2020$ °C a damping $\Gamma=4.0(4)$ meV is observed. This contradicts the intuitive picture that the damping increases on approaching the β to α-phase transition.

We thus argue that the weakness of bcc Hf for displacements toward the ω phase is temperature independent under normal pressure. The large-amplitude fluctuations have to be seen as an intrinsic property of bcc Hf.

B. Transverse phonons with $[\xi\xi 0]$ propagation and $[1\bar{1}0]$ polarization

As argued in I and II,[2,3] the displacements necessary to perform the β-to-α transition can be thought of as a superposition of the transverse N-point phonon with $[1\bar{1}0]$ polarization and the long-wavelength shear $(1\bar{1}2)[\bar{1}11]$. This N-point phonon is the Brillouin-zone boundary phonon of the T_1 $[\xi\xi 0]$ phonon branch. Due to its importance for the phase transition, this phonon branch was measured at several temperatures. Figure 3 gives exam-

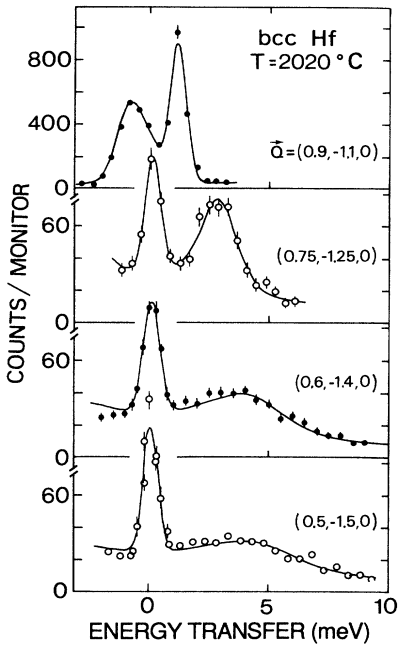

FIG. 3. Phonon groups of the $T_{[1\bar{1}0]}$ [$\xi\xi 0$] branch in bcc Hf at 2020 °C ($k_f = 2.662$ Å^{-1}, otherwise same as Fig. 2). The full line shows fits with a damped oscillator similar to those in Fig. 2.

ples of the phonon groups measured at 2020 °C. Obviously, the T_1 [$\xi\xi 0$] phonons in bcc Hf are broadened and are therefore described by a damped-oscillator function. This broadening is largest for the short-wavelength phonon at the zone boundary. Figure 4 and Table II show the results of these fits. The frequency of the T_1 N-point phonon decreases upon approaching the β-to-α phase transition, thereby indicating the increasing weakness of the bcc lattice for displacements toward the stacking sequence of the hcp structure. Interestingly, the broadening which is also a signature of anharmonicity, shows the inverse behavior dependence compared to the frequency itself, i.e., an increasing weakness with increasing temperature is observed. This corresponds to the observation made for the L $\frac{2}{3}(1,1,1)$ phonon. We therefore conclude that the damping is decoupled from the precursor effects of the β to α transition, merely it is an intrinsitic bcc property, either due to phonon-phonon or phonon-electron coupling.

Similar to results for β-Ti and β-Zr, the phonon dispersion of β-Hf is very anisotropic, i.e., the three-dimensional phonon dispersion surface shows a deep valley ranging from T_1 $\frac{1}{3}(1,1,2)$ [$\doteq$L $\frac{2}{3}(1,1,1)$] to T_1 $\frac{1}{2}(1,1,2)$ [$\doteq T_1$ $\frac{1}{2}(1,1,0)$]. This reveals that the lattice potentials are particularly low for displacements toward the ω or α stacking sequence. Intuitively one argues that these displacements are of particularly large amplitude compared with displacements of other large-q modes. The present harmonic description allows only the calculation of the *isotropic* mean-square displacement, which yields an amplitude of $(\langle u_i^2 \rangle)^{1/2} = 0.28$ Å for Hf at 1800 °C (see Sec. IV). However, it is plausible that the potentials for displacements toward the ω or α phase soften for large displacements and, therefore, allow displacement amplitudes comparable to the shifts needed for the phase transitions. For example, the collapse of the two (1,1,1) planes in the ω phase needs a displacement of a $\sqrt{3}/12 = 0.52$ Å. This hypothesis of strongly anharmonic potentials is supported experimentally by the temperature dependence of the corresponding phonons and theoretically by the frozen phonon calculations of bcc Zr.[7,8] We emphasize that these displacements have a purely dynamical character and that there are no static displacements toward an ω or α structure, i.e., the elastic peak shown in Fig. 2 is of incoherent origin and does not correspond to a superstructure peak.

IV. BORN–VON KÁRMÁN FITS AND RELATED PROPERTIES

In order to get a parametrization of the lattice dynamics, the phonon dispersion measured at 1800 °C was fitted by Born–von Kármán force constants ϕ_{ij}^m up to the fifth-neighbor shell. The fit is shown as a full line in Fig. 1 and the ϕ_{ij}^m are listed in Table III.

According to Eq. (3) of I,[2] the force constants ϕ_{ij}^m are used to calculate the normalized phonon density of states $Z(\omega)$. The result is shown in Fig. 5 and resembles very

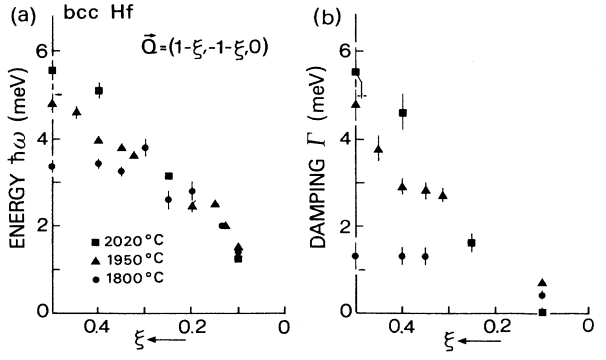

FIG. 4. Temperature dependence of the $T_{[1\bar{1}0]}$ [$\xi\xi 0$] phonon branch in bcc Hf. The results of fits with a damped oscillator, i.e., the center frequency ω_0 and the damping Γ, are shown.

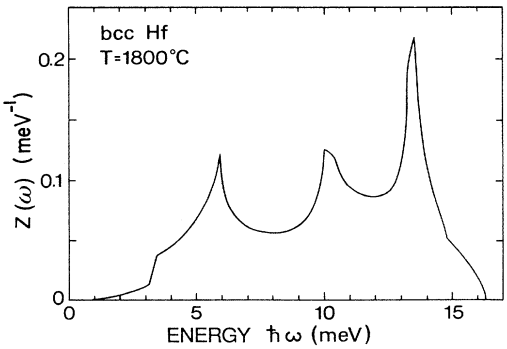

FIG. 5. Phonon density of state $Z(\omega)$ for bcc Hf at 1800 °C as calculated from the measured phonon dispersion.

TABLE III. Force constants ϕ_{ij}^m up to the $m=5$th neighbor shell in dyn/cm obtained from Born von Kármán fits to the dispersion of bcc Hf at 1800 °C (Fig. 1).

m	xx	yy	zz	xy	xz	yz
111	7956	7956	7956	10010	10010	10010
200	5994	−1939	−1939	0	0	0
220	414	414	7.9	−486	0	0
311	1048	173	173	−114	−114	693
222	−378	−378	−378	1084	1084	1084

much those for bcc Ti and bcc Zr. In particular, we mention that the singularity at the lowest energy stems from the low-energy T_1 [$\xi\xi 0$] phonon branch. Because these phonons increase in energy with increasing temperature, this singularity shifts to higher energies, i.e., the lattice stiffens with increasing temperature.

From the density of states $Z(\omega)$, the mean-square displacement $\langle u_i^2 \rangle$ of the atoms, the Debye temperature Θ_D, and the lattice vibrational entropy S_{vib} can be calculated [see Eqs. (4), (5), and (6) of I[2]]. We obtained 0.08 Å for $\langle u_i^2 \rangle$, 145 K for Θ_D, and 11.88 k_B/atom for the S_{vib} in β-Hf at 1800 °C. It has to be emphasized that these quantities are calculated under the assumption of quasiharmonicity. They are correct for 1800 °C at the temperature at which the phonons have been measured. Any harmonic extrapolation to higher temperatures according to Eqs. (4), (5), and (6) of I[2] has to be made with caution. As indicated by the temperature-dependent T_1 [$\xi\xi 0$] phonon branch, the low-energy part of $Z(\omega)$ shifts to higher energies with increasing temperature, i.e., the increase of $\langle u_i^2 \rangle$ with temperature is reduced. In the same way, the increase of $S_{\text{vib}}(T)$ with increasing temperature is slowed down and Θ_D does not stay constant but increases with increasing temperature. It is not possible to estimate the excess lattice entropy at the β to α transition, because phonon measurements of α-Hf at high temperature are not available and harmonic extrapolations from room-temperature data are not reliable enough. The elastic constants at 1800 °C are calculated from the force constants ϕ_{ij}^m (Ref. 9) and yield $C_{11}=1.31$, $C_{12}=1.03$, and $C_{44}=0.45$ in units of 10^{12} dyn/cm^2. Similar to its chemical homologs, β-Hf is very anisotropic with respect to its dynamical behavior.

V. COMPARISON OF THE PHONON ANOMALIES OF GROUP-IV METALS

In general the phonon dispersions of the bcc structure of group-IV metals resemble very much each other and are dominated by the extraordinary low energy of the L $\frac{2}{3}(1,1,1)$ mode and the T_1 [$\xi\xi 0$] phonon branch. Figure 6(a) compiles this information. All phonons which are not of particular low energy show a variation of their frequency for the different elements which follow classical behavior, i.e., may be scaled by $1/(\sqrt{m}\,.a)$ to a common dispersion. This is not the case for the L $\frac{2}{3}(1,1,1)$ phonon mode and the T_1 [$\xi\xi 0$] phonon branch. These modes are damped for all three elements and in spite of the different masses they are of similar low energy. Those of β-Ti seem to be of higher frequency. This is a result of the assumed model of an overdamped oscillator, i.e., the fitted center frequency is shifted with respect to the energy of the highest count rate (see Fig. 7).

In none of the three elements Ti, Zr, and Hf does the L $\frac{2}{3}(1,1,1)$ phonon energy change with temperature. It is concluded that the weakness toward ω fluctuations is an

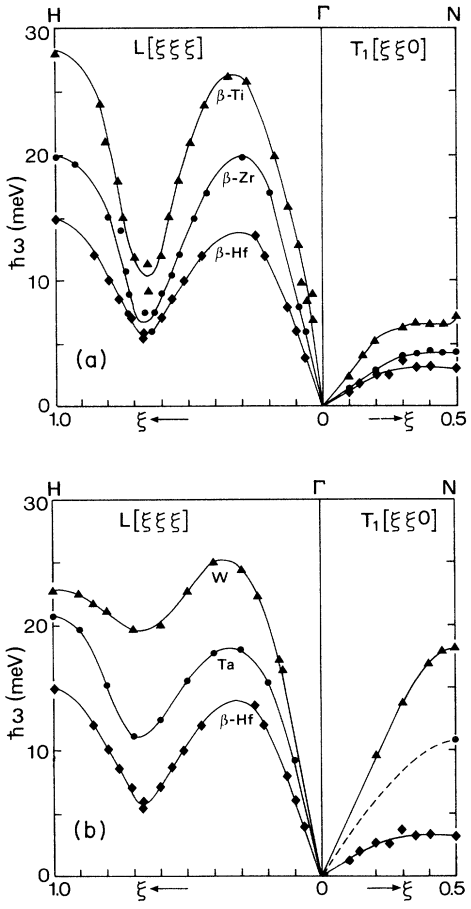

FIG. 6. Comparison of the L [$\xi\xi\xi$] and $T_{[1\bar{1}0]}$ [$\xi\xi 0$] phonon branch for the bcc phase of (a) the group-IV metals with 2 d electrons and (b) of metals with a variation of the d-electron density from 2 to 4. Data stem from Refs. 2, 3, and 11. For β-Ti, β-Zr, and β-Hf data measured close to the β to α transition have been chosen, all other measurements refer to room temperature.

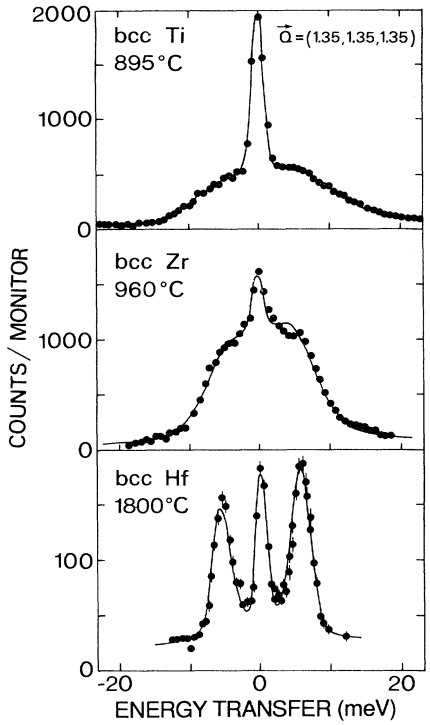

FIG. 7. Energy scans at constant $\mathbf{Q}=1.35(1,1,1)$ for bcc Ti, bcc Zr and bcc Hf at temperatures some 60 °C above T_0. Hf has been measured with 50′-20′-40′-40′ collimation, $k_f=4.1$ and a PG(004) analyzer.

intrinsic property of group-IV metals caused by the rather open bcc structure (see also I,[2] Sec. III A). In the case of group-IV elements, this geometrical weakness is enhanced by *d* bonds along [111] chains.[8] With increasing *d*-electron density, these *d* bonds entangle the [111] chains and give rise to forces which oppose the shearing motion of the [111] chains as they are performed by the L $\frac{2}{3}(1,1,1)$ phonon.[10] This picture of the *d*-electron density as the relevant control parameter is illustrated in Fig. 6(b) where the degree of softening of the L $\frac{2}{3}(1,1,1)$ phonon scales with the decreasing *d*-electron density whereas for all group-IV metals the L $\frac{2}{3}(1,1,1)$ mode is of comparable low frequency.

We have no real understanding from first principles why these low-energy phonons are so strongly damped (though to a lesser extent in β-Hf). Figure 7 compares the broad intensity distribution in energy of the L $\frac{2}{3}(1,1,1)$ mode for the three transition elements with two *d* electrons. The damping systematically decreases with increasing mass. This is expected from classical considerations where—given a constant friction term—the damping is proportional to the inverse of the mass.

Whereas in β-Ti and β-Zr the line broadening or damping of these low-energy phonons is constant over the whole temperature range of the bcc phase, the damping increases in β-Hf with increasing temperature. The fact that the damping of the T_1 *N*-point phonon is constant or smaller close to T_0 supports the argument that the damping is not directly related to the β- to α-phase transition but merely a characteristic of the bcc phase of the group-IV metals itself.

VI. CONCLUSION

The phonon dispersion of bcc Hf is dominated by the fact that it transforms under pressure to the ω structure and to hcp upon decreasing the temperature. The T_1 *N*-point phonon, which shifts the bcc (1,1,0) planes toward the stacking sequence of hcp, is of low energy (i.e., of large amplitude). Furthermore, its amplitude increases upon approaching the β-to-α transition and is therefore a kind of dynamical precursor of the martensitic transition. Thus, β-Hf resembles very much its chemical homologs β-Ti and β-Zr (see I[2] and II[3]).

The L $\frac{2}{3}(1,1,1)$ mode, which displaces the (1,1,1) planes toward the hexagonal ω structure is of low frequency, as well. Different from β-Ti and β-Zr, this mode is only weakly damped at the transition temperature. By interpreting the damped ω phonon in the equivalent picture of a distribution of low-energy excitations, these excitations are less sluggish in β-Hf than in β-Ti or β-Zr. Macroscopically, this might reflect the higher pressure needed to achieve the ω structure.

Summarizing our study on the lattice dynamics of three group-IV metals, we emphasize the role of low-energy phonons as dynamical precursors of the displacive phase transitions. The temperature dependence of T_1 $[\xi\xi 0]$ phonon frequencies yields critical elongations at the phase-transition temperature which destabilizes the bcc structure. The difference in free energy, which is dominated by the changes of vibrational entropy (see II[3]), drives a uniform transformation involving the entire crystal. This view is supported by first-principles total-energy calculation on similar systems.[12]

With respect to the kinetics of the phase transition, we state that there exists no static precursors, such as central peaks or static embryos of the new low-temperature phase. Systems in which these phenomena have been observed are either in a two-phase region (see discussion of β-Zr/α-ZrO in II[3] or their transformation is dominated by intrinsic heterophase nucleations. In the latter case, static precursors could be interpreted as seeds of the developing phase which grow with decreasing temperature.[13]

ACKNOWLEDGMENTS

Financial support given by the German Bundesministerium für Forschung und Technologie, under Project No. 03-HE2MUE-0 is gratefully acknowledged.

[1]S. K. Sikka, Y. K. Vohra, and R. Chidambaram, Progr. Material Sci. **27**, 245 (1982).

[2]W. Petry, A. Heiming, J. Trampenau, M. Alba, C. Herzig, H. R. Schober, and G. Vogl, Phys. Rev. B **43**, 10 933 (1991) (referred to hereafter as I); W. Petry, A. Heiming, J. Trampenau, M. Alba, and G. Vogl, Phys. Rev. Lett. **61**, 722 (1988); W. Petry, A. Heiming, J. Trampenau, M. Alba, and G. Vogl, Physica B **156&157**, 56 (1989).

[3]A. Heiming, W. Petry, J. Trampenau, M. Alba, C. Herzig, H. R. Schober, and G. Vogl, Phys. Rev. B **43**, 10 948 (1991) (referred to hereafter as II); A. Heiming, W. Petry, J. Trampenau, M. Alba, C. Herzig, and G. Vogl, Phys. Rev. B **40**, 11 425 (1989).

[4]For a compilation of phase diagrams and thermodynamic properties of gaseous impurities in group-IV metals, see Gase und Kohlenstoff in *Metallen,* edited by E. Fromm and E. Gebhardt (Springer-Verlag, Berlin, 1976).

[5]Based on our own measurements and those of R. G. Ross and W. Hume Rothery, J. Less Common Met. **5**, 258 (1963).

[6]Homology assumes that the lattice potential scales with the lattice parameter $V(r)=v(r/a)$.

[7]K.-M. Ho, C. L. Fu, and B. N. Harmon, Phys. Rev. B **28**, 6687 (1983); **29**, 1575 (1984).

[8]Y. Chen, C. L. Fu, K.-M. Ho, and B. N. Harmon, Phys. Rev. B **31**, 6775 (1985).

[9]G. L. Squires, in *Proceedings of the Symposium on Inelastic Scattering of Neutrons in Solids and Liquids, Chalk River, 1962* (IAEA, Vienna, 1963), Vol. II, p. 71.

[10]K.-M. Ho, C. L. Fu, and B. N. Harmon, Phys. Rev. B **28**, 6687 (1983).

[11]H. R. Schober and P. H. Dedrichs, in Landolt-Börnstein, New Series, Group III, (Springer, Berlin, 1981) Vol. 13a, and references cited therein.

[12]K.-M. Ho and B. N. Harmon, Mater. Sci. Eng. A **127**, 155 (1990).

[13]W. Cao, J. A. Krumhansl, and R. J. Gooding, Phys. Rev. B **41**, 11 319 (1990).